

# The MHD nature of ionospheric wave packets excited by the solar terminator

E.L. Afraimovich, S.V. Voeikov, I.K. Edemskiy, Yu.V. Yasyukevich

Institute of Solar-Terrestrial Physics SB RAS, Irkutsk, Russia,  
p.o. box 291, 664033, fax: +7 3952 511675.

e-mail: ilya@iszf.irk.ru

September 29, 2018

## Abstract

We obtained the first experimental evidence for the magnetohydrodynamic (MHD) nature of ionospheric medium-scale travelling wave packets (MSTWP). We used data on total electron content (TEC) measurements obtained at the dense Japanese network GPS/GEONET (1220 stations) in 2008-2009. We found that the diurnal, seasonal and spectral MSTWP characteristics are specified by the solar terminator (ST) dynamics. MSTWPs are the chains of narrow-band TEC oscillations with single packet's duration of about 1-2 hours and oscillation periods of 10-20 minutes. Their total duration is about 4–6 hours. The MSTWP spatial structure is characterized by a high degree of anisotropy and coherence at the distance of more than 10 wavelengths. The MSTWP direction of travelling is characterized by a high directivity regardless of seasons. Occurrence rate of daytime MSTWPs is high in winter and during equinoxes. Most of daytime MSWPs propagate southeastward ( $155 \pm 28^\circ$ ) at the velocity of  $130 \pm 52$  m/s. Occurrence rate of nighttime MSTIDs has its peak in summer. They propagate southwestward ( $245 \pm 15^\circ$ ) at the velocity of  $110 \pm 43$  m/s. These features are consistent with previous MS travelling ionosphere disturbance (TID) statistics obtained from 630-nm airglow imaging observations in Japan. In winter, MSTWPs in the northern hemisphere are observed 3-4 hours after the morning ST passage. In summer, MSTWPs are detected 1.5-2 hours before the evening ST occurrence at the point of observations, at the moment of the evening ST passage in the magneto-conjugate point. Both the high Q-factor of oscillatory system and synchronization of MSTWP occurrence with the solar terminator passage at the point of observations and in the magneto-conjugate area testify the MHD nature of ST-excited MSTWP generation. The obtained results are the first experimental evidence for the hypothesis of the ST-generated ion sound waves.

## 1 Introduction

Pioneering theoretical works of V.M. Somsikov ((1995) and other papers) marked the beginning of numerous experimental observations of "terminator" waves with the use of different methods of ionospheric radio sounding. Recent investigations have shown that movement of the solar terminator (ST) causes generation of acoustic-gravity waves (AGW), turbulence and instabilities in the ionosphere plasma. It is worth noting that among all the sources of gravity waves, the moving ST has a special status, since it is a predictable phenomenon whose characteristics are well known. Considering the ST as a stable and repetitive source of AGWs, one can derive information about atmospheric conditions from the response of the medium to this input. The great variety of ST-linked phenomena in the atmosphere gave rise to a number of studies on the analysis of ionosphere parameter variations obtained by different methods of ionosphere sounding [Drobzhev et al., 1992; Hocke and Schlegel, 1996; Dominici et al., 1997; Galushko et al., 1998]. However, virtually all experimental data were obtained using indirect methods for analyzing the spectrum of ionosphere parameter variations, which can

result from a number of factors. This causes difficulties in the reliable identification of ST AGWs, because in general case AGWs can be generated by different sources either of natural or of anthropogenic origin [Hocke and Schlegel, 1996].

Recently a considerable progress has been achieved in the study of ionosphere irregularities using the new technology of GPS radio sounding. It allows us to obtain the data on variations of the total electron content (TEC) with high spatial and temporal resolution. Afraimovich (2008) has obtained the first GPS TEC evidence for the wave structure excited by the morning ST, moving over the USA, Europe, and Japan. The author has first found ST-generated medium-scale travelling wave packets (MSTWP). These MSTWPs have duration of about 1-2 hours and time shift of about 1.5-2.5 hours after the morning ST appearance at the altitude of 100 km.

Registering time dependence of ionosphere parameters is insufficient to identify ST-generated wave disturbances. It is necessary to determine the spatial structure of these disturbances and compare it with the spatial-temporal characteristics of ST. Hence, it is very important to define the spatial structure of MS wave packets in TEC. Using TEC measurements from the dense network of GPS sites GEONET, Afraimovich et al. (2009) has obtained the first GPS-TEC image of the space structure of MSTWP excited by the morning ST motion of ST on 13 June 2008.

The goal of this paper is to obtain the detailed information regarding the spatial, spectral and dynamic characteristics of MSTWPs excited by the ST as deduced from the dense GPS network GEONET.

## 2 Data and Methods

We use data from the Japanese GPS network GEONET (about 1225 stations in total). Actually, it is the world's largest regional GPS network<sup>†</sup>. The geomagnetic situation on selected and analyzed days of 2008-2009 can be characterized as quiet: the Kp index varied from 1.0 to 3.0.

The standard GPS technology provides a means of detection of wave disturbances based on phase measurements of TEC at each of two-frequency spaced GPS receivers [Calais et al., 2003; Afraimovich et al., 2003; Hernandez-Pajares et al., 2006]:

$$I_o = \frac{1}{40.308} \frac{f_1^2 f_2^2}{f_1^2 - f_2^2} [(L_1 \lambda_1 - L_2 \lambda_2) + const + nL], \quad (1)$$

where  $L_1 \lambda_1$  and  $L_2 \lambda_2$  are additional paths of the radio signal caused by the phase delay in the ionosphere, (m);  $L_1$  and  $L_2$  represent the number of phase rotations at the frequencies  $f_1$  and  $f_2$ ;  $\lambda_1$  and  $\lambda_2$  stand for the corresponding wavelengths, (m); *const* is the unknown initial phase ambiguity, (m); and  $nL$  are errors in determining the phase path, (m). Phase measurements in GPS can be made with a high degree of accuracy corresponding to the error of TEC determination of at least  $10^{14} \text{ m}^{-2}$ , when averaged on a 30-second time interval, but with some uncertainty of the initial value of TEC. This allows us to detect ionization irregularities and wave processes in the ionosphere over a wide range of amplitudes (up to  $10^{-4}$  of the diurnal TEC variation) and periods (from 24 hours to 5 min). The total electron content unit (TECU) equal to  $10^{16} \text{ m}^{-2}$  and commonly accepted in the literature will be used below.

Primary data include series of "oblique" values of TEC  $I_o(t)$ , as well as the corresponding series of elevations  $\theta_s(t)$  and azimuths  $\alpha_s(t)$  of the line of sight (LOS) to the satellite.

Series of values of elevations  $\theta_s(t)$  and azimuths  $\alpha_s(t)$  of LOS to the satellite was used to determine coordinates of subionospheric points (SIP) for the height  $h_{max}=300$  km of the  $F_2$ -layer maximum and to convert the "oblique" TEC  $I_o(t)$  to the corresponding value of the "vertical" TEC

$$I = I_o \times \cos \left[ \arcsin \left( \frac{R_z}{R_z + h_{max}} \cos \theta_s \right) \right], \quad (2)$$

where  $R_z$  is the Earth's radius. All results in this study were obtained for elevations  $\theta_s(t)$  larger than  $50^\circ$ .

To eliminate variations in the regular ionosphere, as well as trends introduced by orbital motion of the satellite, we derive TEC variations  $dI(t)$  by filtering from the initial  $I(t)$ -series over the range of periods of 2-20 min.

---

<sup>†</sup>[ftp://terras.gsi.go.jp/data/GPS\\_products/](ftp://terras.gsi.go.jp/data/GPS_products/)

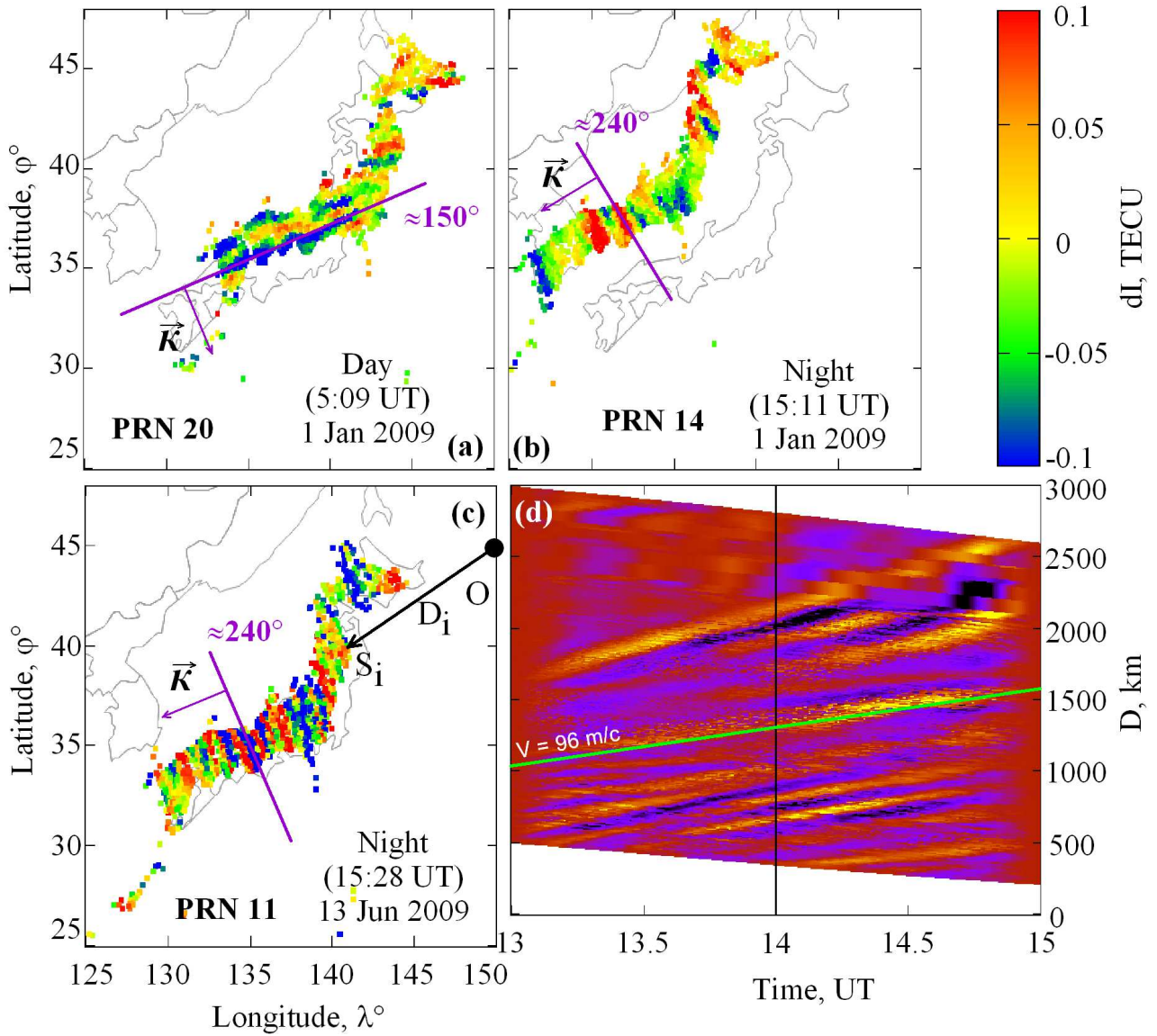


Figure 1: The latitude-longitude 2D-space distribution of the filtered TEC  $dI$  ( $\varphi$ ,  $\lambda$ ) after morning ST passage over Japan on 1 January 2009, 05:09 UT (a); after evening ST on 1 January 2009, 15:11 UT (b); and after evening ST on 13 June 2008, 15:28 UT (c). (d) - TWPs for all GPS sites located along the direction  $D$  over Japan for selected satellite number PRN19 on 13 June 2008, 13:00-15:00 UT. The velocity  $V$  of TWPs is defined through the inclination of the wave front line (the green line on the panel (d)).

### 3 TWP spatial characteristics

We use two known forms of the 2D GPS-TEC imaging for our presentation of the ST-generated MSTWP space structure. First we apply the diagram "distance-time"  $dI(t, D)$  used by different authors [Calais et al., 2003; Afraimovich et al., 2009]. This diagram is calculated in the polar coordinate system (Fig. 1c). Points 0 and  $S_i$  mark the relative coordinate centre and the SIP position for LOS between the GPS site with number  $i$  and the selected satellite PRN, respectively;  $D_i$  is the distance between points 0 and  $S_i$  along the great circle arc. Here we select the geographic latitude and longitude for point 0 ( $45^\circ\text{N}$  and  $150^\circ\text{E}$ ) outside the GEONET GPS sites field. This location of the relative coordinate center is chosen to make more adequate correspondence between

distance to each GPS site and its actual location.

Neglecting the Earth's sphericity, we can determine coordinates  $x_i(t)$  and  $y_i(t)$  of the SIPs  $S_i$  at an altitude  $h_{max}$  in the topocentric coordinate system with the center in GPS as

$$\begin{aligned} x_i(t) &= h_{max} \sin(\alpha_i(t)) \cot(\theta_i(t)) \\ y_i(t) &= h_{max} \cos(\alpha_i(t)) \cot(\theta_i(t)) \end{aligned} \quad (3)$$

where  $\alpha_s$  is the azimuth counted off from the north in a clockwise direction;  $\theta_s$  is the LOS elevation [Afraimovich et al., 2003].

Then we recalculate topocentric coordinates  $x_i(t)$  and  $y_i(t)$  into corresponding values of the latitude  $\varphi$  and longitude  $\lambda$  of SIPs  $S_i$ , calculate distance  $D_i$  and then plot the 2D-diagram "distance-time"  $dI(t, D)$  for the selected satellite number PRN. Our approximation is acceptable only for large  $\theta_i$  values. So for the minimum  $\theta_i$  value of about  $45^\circ$  and  $h_{max} = 300$  km, the maximum deviation of SIPs  $S_i$  from GPS site does not exceed 300 km.

In order to study space properties and dynamics of TWP packets in detail, we also employ another form of the 2D-space distribution of values of filtered TEC series  $dI(\varphi, \lambda)$  in latitude  $\varphi$  and longitude  $\lambda$  for each 30-sec TEC counts with spatial resolution of  $0.15^\circ$  in latitude and  $0.15^\circ$  in longitude. Then we build up the dynamic image of disturbances travelling over Japan in video format (AVI). Similar technology was first developed by Saito et al.(1998). Authors showed that a high-resolution two-dimensional mapping of TEC perturbations at the GPS GEONET network revealed spatial and temporal TEC variations at mid-latitudes in detail. This had never been attained in the past. The said space-time presentation method of ionosphere disturbances for the dense GPS networks of USA was used in [Tsugawa et al., 2007].

Fig. 1 presents the latitude-longitude 2D-space distribution of the filtered TEC  $dI(\varphi, \lambda)$  after the morning ST passage over Japan on 1 January 2009, at 05:09 UT (a); after the evening ST on 1 January 2009, at 15:11 UT (b); and after the evening ST on 13 June 2008, at 15:28 UT (c). The amplitude of  $dI(t)$  variations is about 0.1 TECU (scale for  $dI$  is plotted on the panel (b) at the right). Lines mark the wave front extension; numbers near lines mark direction  $\alpha$  of the MSTWP wave vector  $\mathbf{K}$ :  $150^\circ$  for 1 January 2009 (05:09 UT),  $240^\circ$  for 1 January 2009 (15:11 UT) and  $240^\circ$  for 13 June 2008 (15:28 UT), respectively.

Fig.1(d) presents the 2D-diagram "distance-time"  $dI(t, D)$  for TWPs on 13 June 2008, for GPS sites located along the direction  $D$  over Japan for satellite number PRN19 at 13:00-15:00 UT. The velocity  $V=96$  m/s of TWPs is defined through the inclination of the wave front line (the green line on the panel (d)). Vertical line marks the time moment 15:28 UT (see the corresponding 2D-space distribution  $dI(\varphi, \lambda)$  on the panel (c)).

We have analyzed a number of similar images of MS TWP spatial structure over Japan. The MS TWP space image is characterized by pronounced anisotropy (ratio between the lengthwise and transversal scales exceeds 10) and high coherence over a long distance of about 2000 km. The MS TWP wavelength varies from 100 km to 300 km. Spatial structure of 2D-space distribution  $dI(\varphi, \lambda)$  remain stable along whole Japan at the distance of up to 2000 km.

## 4 Dynamic characteristics of TWPs by the SADM-GPS method

In order to determine velocity of TIDs, we use method taking into account the relative motion of SIPs into account [Afraimovich et al., 1998, 2003]. We determine velocity and direction of the wave front motion in terms of some model, whose adequate choice is of crucial importance. In the simplest form, space-time variations in TEC variations  $dI(t, x, y)$  at each given moment of time  $t$  can be represented in terms of the phase pattern that moves without any change in its shape (non-dispersive disturbances):

$$I(t, x, y) = F(t - x/u_x - y/u_y) \quad (4)$$

where  $u_x(t)$  and  $u_y(t)$  are displacement velocities of intersection of the phase front of axes  $x$  and  $y$ , respectively;  $F$  is an arbitrary function.

A special case of (4) is the most often used model for a solitary plane travelling wave of the TEC disturbance

$$I(t, x, y) = \delta \sin(\Omega t - K_x x - K_y y + \varphi_0) \quad (5)$$

where  $\delta$ ,  $K_x$ ,  $K_y$ ,  $\Omega$  are the amplitude, the  $x$ - and  $y$ - projections of the wave vector  $\mathbf{K}$ , and the angular frequency of the disturbance, respectively;  $\varphi_0$  is the initial disturbance phase.

A SADM-GPS method was proposed by Afraimovich et al. (2003) for determining the TID dynamics in the horizontal plane by measuring variations of TEC derivatives with respect to the spatial coordinates  $I'_x(t)$ ,  $I'_y(t)$  and to the time  $I'_t(t)$ . This allows us to determinate the unambiguous  $\alpha(t)$  orientation of the wave-vector  $\mathbf{K}$  over the range of 0–360° and the horizontal velocity  $V(t)$  at each specific instant of time. A detailed description of the method is presented in [Afraimovich et al. 2003].

Let us take a brief look at the sequence of data handling procedures. Out of a large number of GPS stations, three points ( $A, B, C$ ) are chosen in such a way that the distances between them do not exceed about a half of the expected wavelength  $\Lambda$  of the disturbance. The point  $B$  is considered as the center of the topocentric frame of reference. Such configuration of GPS receivers represents a GPS-array (or a GPS-interferometer) with the minimum of the necessary number of elements. In regions with a dense network of GPS-points, we can obtain a broad range of GPS-arrays of a different configuration, which provides a means for testing the data obtained for reliability; in this paper we took advantage of this possibility.

The input data include series of vertical TEC  $I_A(t)$ ,  $I_B(t)$ ,  $I_C(t)$ . Linear transformations of the differences between values of filtered TEC variations ( $dI_B - dI_A$ ) and ( $dI_B - dI_C$ ) at the receiving points A, B and C are used to calculate the components of the TEC gradients  $I'_x$  and  $I'_y$ .

The resulting series are used to calculate instantaneous values of the horizontal velocity  $V(t)$  and the azimuth  $\alpha(t)$  of TID propagation. Next, the series  $V(t)$  and  $\alpha(t)$  are put to a statistical treatment. This involves construction of distributions of the horizontal velocity  $P(V)$  and direction  $P(\alpha)$ , which are analyzed to test the hypothesis of the existence of the preferred propagation direction. If such a direction does exist, the corresponding distributions are used to calculate the mean values of the horizontal velocity  $\langle V \rangle$  and azimuth  $\langle \alpha \rangle$  of TID propagation. Using different sets of  $n$  GPS arrays, we managed to obtain average values of the horizontal projection  $V$  and direction  $\alpha$ .

Fig. 2. presents the examples of the distributions of the MSTWP dynamics parameters for nighttime of 13 June 2008, 13-15.3 UT (**a**),  $n=387$ ; for daytime of 1 January 2009, 03-05.3 UT (**b**),  $n=344$ ; and for daytime of 13 June 2008, 05-7.3 UT (**c**),  $n=440$ ; azimuth  $\alpha$  - at the left, and horizontal component of MSTWP travelling velocity  $V$  - at the right. Events (**a**) and (**b**) correspond to the strongly directional travelling of MSTWPs for nights and days; the mean value and RMS of the azimuth  $\alpha$  equal 240° and 10°, and 165° and 19°, respectively. The event (**b**) illustrates a total absence of directional TWPs travelling. In all events, the velocity  $V$  does not exceed 250-300 m/s. The mean value and RMS of  $V$  equal 118 and 28 m/s for the night; 146 and 49 m/s for the day, and 135 and 49 m/s for nondirectional travelling, respectively.

The hypothesis of the connection between wave packet generation and ST appearance can be tested in the terminator local time ( $TLT$ ) system:  $dT = t_{obs} - t_{st}$ , where  $t_{obs}$  is the data point time, and  $t_{st}$  is the time of ST appearance at the altitude of  $H$  over this point. In other words, firstly we transformate the latitude and longitude of the point to a time of the terminator appearance over this point and then we define the difference between the terminator appearance time and the time at the data point. A distinctive feature of this approach is in excluding the point coordinates and considering each point data in the solar terminator context only [Afraimovich et al., 2009]. Of the greatest interest is total diurnal distributions of travelling direction  $\alpha$  for summer 2008 (Fig. 3. (**a**)) and winter 2009 (Fig. 3. (**e**)) versus the local terminator time  $dT$ . 2D- distributions of the azimuth  $\alpha$  are calculated using data from  $n=492590$  GPS-arrays for (**a**); and  $n=197150$  for (**e**). The numbers on the panels mark the numbers of the analyzed days for the summer and winter. The steps on  $TLT$   $dT$  and azimuth  $\alpha$  equal 0.5 h and 5°, respectively. The scale for number of count hits  $N$  in different bins of distributions is plotted on panels (**a**) and (**e**) at the right.

The total distribution in Fig.(**a**) corresponds to the strongly directional travelling of MSTWPs at the night for full 35 summer days; the mean value and RMS of the azimuth  $\alpha$  equal 240° and 10°, respectively. The strongly directional travelling begins immediately after the sunset (SS) ST appearance at observational points and continues for about 5 h. A similar picture is also significant for the night for full 16 winter days (Fig.(**e**)); the mean value and RMS of the azimuth  $\alpha$  equal 240° and 10°, respectively. But in this case the strongly directional travelling begins 5 h after SS ST appearance at observation points and continues for about 5 h. For the day, the strongly directional travelling of MSTWPs corresponds to the mean value and RMS of the azimuth  $\alpha$  equal to 160° and 10°, respectively. It starts 4 h after the sunrise (SR) ST appearance at observation points and continues for about 3-4 h. Beyond the mentioned time intervals is a total absence of directional TWP

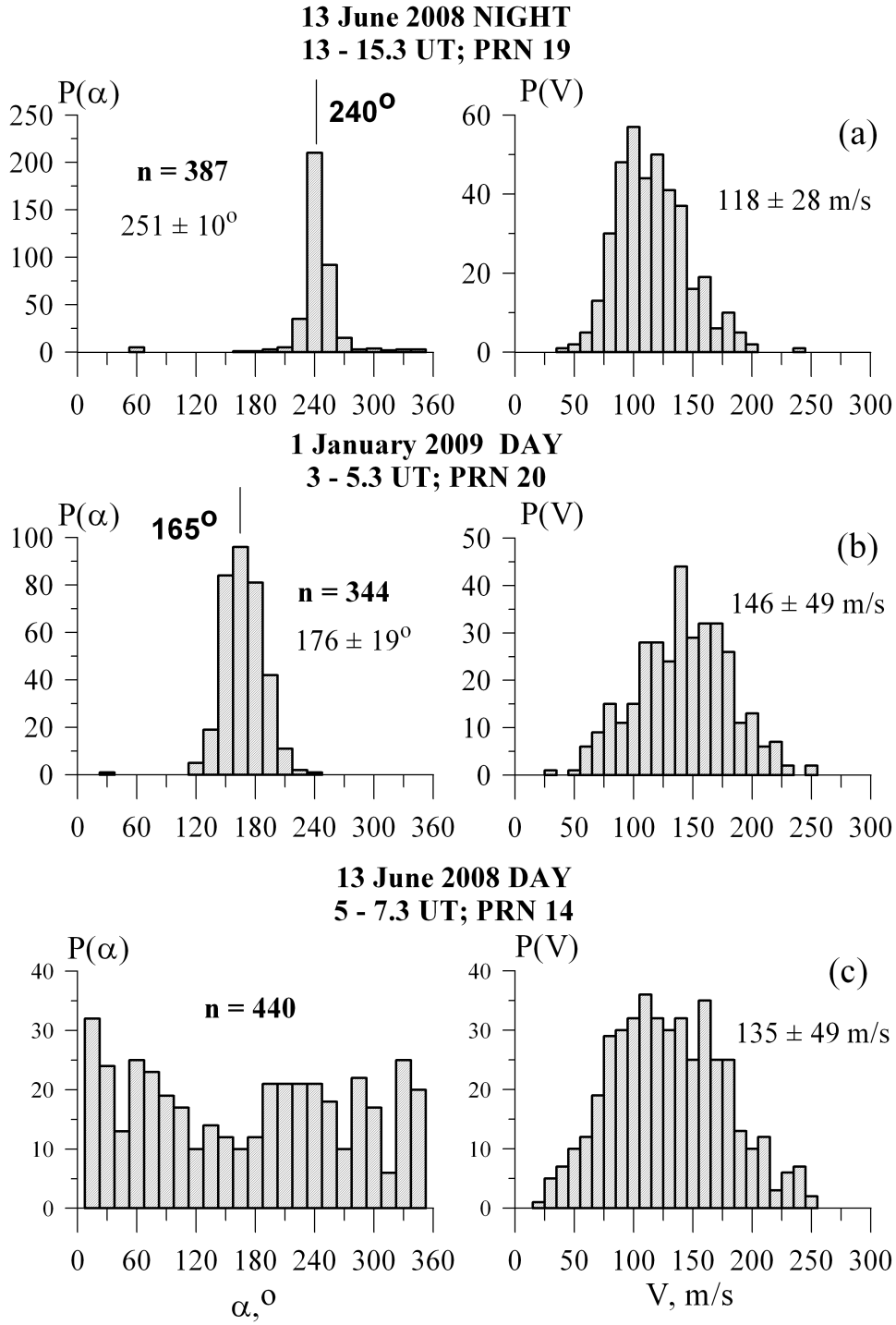


Figure 2: Distributions of the TWP parameters for the nighttime of 13 June 2008 (a), for the daytime of 1 January 2009 (b), and for the daytime of 13 June 2008 (c), as determined by the SADM-GPS method; azimuth  $\alpha$  - at the left, and horizontal component of TWP travelling velocity  $V$  - at the right. Events (a) and (b) correspond to the strongly directional travelling of TWPs at the night and the day; the event (b) illustrates the absence of directional TWPs travelling.

travelling.

As we have found out, two types of MSTWPs - regular and chaotic ones - are observed for 24 hours. The regular travel with duration of some hours is synchronized with the ST passage. "Day" and "night" values of the TWP wave vector direction in the regular motion stage are securely fixed and independent of a season and terminator front direction.

## 5 TWP spectrum and ST appearance over observational and magneto-conjugate points

Main characteristics of wave processes are temporal and spatial spectra. A calculation of a single spectrum of TEC variations involves continuous series of  $dI(t)$  with duration of no less than 2.3 hours, thus enabling us to obtain a number of counts equal to 256 that is convenient for the algorithm of the fast Fourier transform (FFT) used in this study. Before spectral analysis procedure, series  $dI(t)$  are obtained by filtering from the initial  $I(t)$ -series over the range of periods of 2-30 min. To improve the statistical validity of the data, we use the method involving a regional spatial averaging of TEC disturbance spectra for all GPS/GEONET sites.

Figs. 3(b), (c), (d) present the dynamic spectra of TWPs versus the local terminator time  $dT$  for the sunset (SS) ST passing over the point of observation and for SS over the magneto-conjugate point (MCSS). The dynamic spectra are calculated using  $N$  counts for each bins of spectra (total number of  $dI(t)$  data series  $m=3687173$  for (b);  $m=2059177$  for (c);  $m=1656426$  for (d)). The numbers on the panels mark the numbers of the analyzed days for the summer 2008 ((b); for the autumn 2008 (c), and for the winter 2009 ((d). The steps on TLT  $dT$  and variation frequency  $F$  equal 0.5 h and 0.13 mHz, respectively. The amplitude of spectral components is of about 0.02–0.1 TECU (scale for  $dI$  is plotted at the right).

According to the dynamic spectra, MSTWPs are the chain of narrow-band TEC oscillations with individual packet's duration of about 1-2 hours and oscillation periods of 10-20 minutes. Its total duration is about 4–6 hours.

The most important discovery is that TWPs in Japan in summer are registered 1.5-2 hours before the ST appearance over the registration point, when the evening ST passes over the magneto-conjugate point in Australia (b). At the equinox, those moments (SS and MCSS) contemporize (c); in winter TWPs are recorded 4-6 hours after the evening SS and MCSS moments (d).

It is very interesting to compare  $TLT$  dependencies of MSTWP spectrum with similar dependencies of the azimuth  $\alpha$  (Fig. 3(a), (e)). The strongly directional travelling begins after MSTWP appearance and continues over less time interval than the MSTWP appearance in spectra.

## 6 Discussion

Our observations confirm that the ST is a stable and repetitive source of ionospheric wave disturbances. Besides, we confirm the validity of the discovery of ST wave packets made by Afraimovich (2008). The obtained results are in agreement with the theoretical indications of solar terminator effects [Somsikov, 1995] and do not contradict the results obtained by Drobzhev et al. (1992) and Dominici et al. (1997), which are based on limited statistical material. Drobzhev et al. (1992) studied the dynamic spectra of the radio-wave reflection virtual heights obtained by the vertical sounding of the ionosphere. It was shown that during transient hours of the day under magnetically quiet conditions, the low-frequency maximum of the spectra shifted to the higher-frequency region.

Our main results agree with the data on the MSTID spatial structure, dynamics and spectrum variations from different methods of ionosphere radio sounding [Drobzhev et al., 1991, 1992; Jacobson et al., 1995; Mercier, 1996; Hocke and Schlegel, 1996; Dominici et al., 1997; Galushko et al., 1998; Saito et al., 1998; Calais et al., 2003; Afraimovich et al., 1998, 1999, 2003; Hernandez-Pajares et al., 2006; Kotake et al., 2007; Tsugawa et al., 2007]. Kotake et al. (2007) first showed statistical characteristics of the MSTIDs over Southern California observed with densely spaced GPS receivers, and found that characteristics of MSTIDs varied in daytime, dusk, and nighttime.



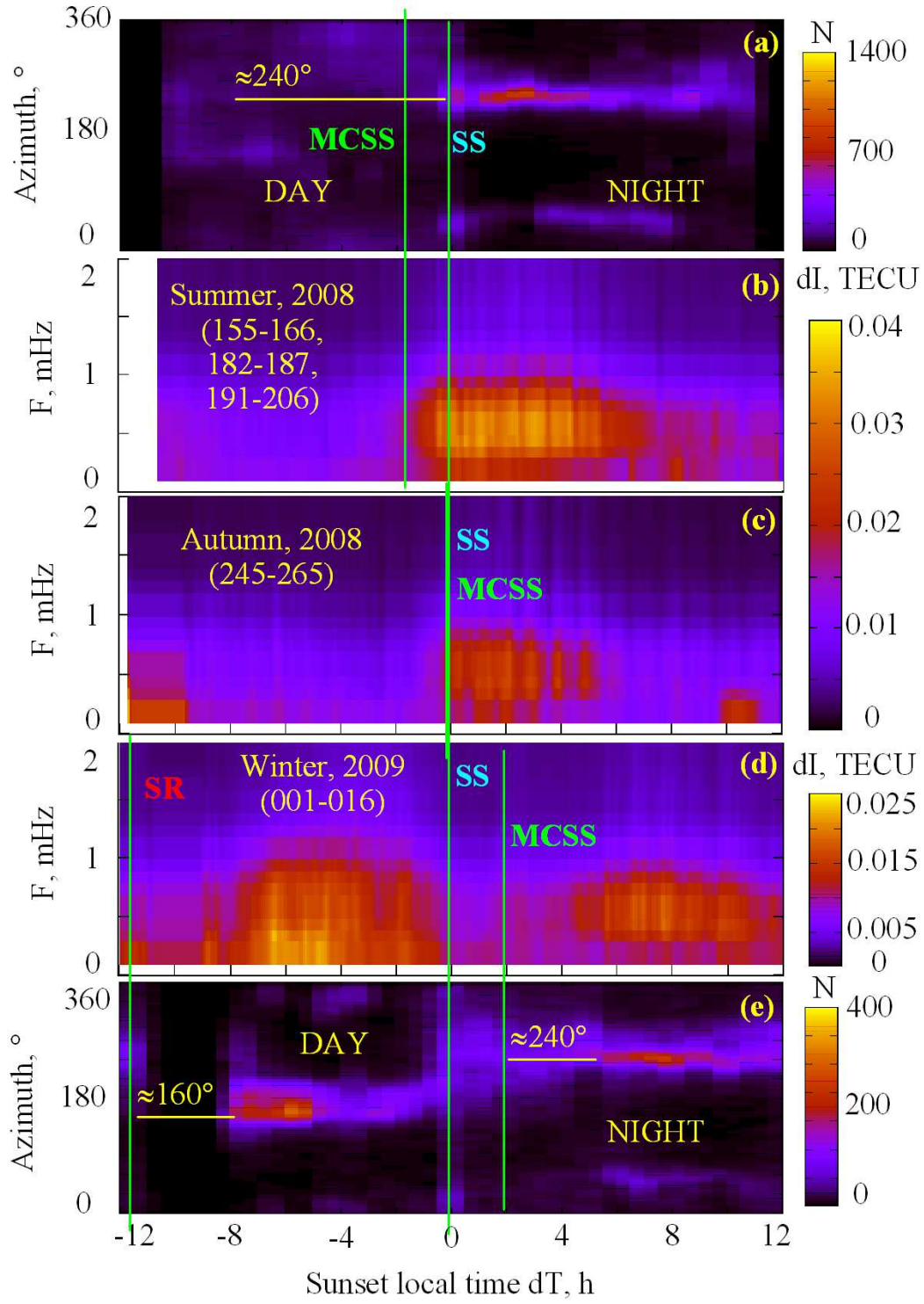


Figure 3: (b), (c), (d) - the dynamic spectra of TWPs versus the local terminator time  $dT = t_{obs} - t_{st}$  between the time of observation  $t_{obs}$  and the time  $t_{st}$  of sunset (SS) ST passing over the observation points. (a), (e) - similar dependencies of the azimuth  $\alpha$  versus the local terminator time  $dT$ . Vertical lines MCSS mark the moments of SS ST passage over the magneto-conjugate point.



On the other hand the recent advent of new observation techniques using all-sky CCD imagers brought about new insights into the two-dimensional properties of TIDs. In Japan there is a network of 630.0 nm (OI) airglow imagers. Our results regarding the MSTWP spatial structure and dynamics check well with the data from all-sky CCD imagers [Ogawa et al., 2002; Otsuka et al., 2004; Shiokawa et al., 2003, 2005].

The question about the mechanism of the observed TEC oscillation is still unclear. MSTIDs (including those dependent on the terminator) are traditionally connected with modulation of the electron density of AGWs generated in the lower atmosphere as the terminator passes over the observation point. However, this hypothesis is not in agreement with characteristics of terminator waves we have found out (a high spatial coherence, strong anisotropy, stable directions of the wave vector azimuth). It is known that AGWs and TIDs can propagate without significant attenuation and changes in their shape or loss of their coherence no farther than 3-5 wavelengths; MSTIDs can propagate within 500-1000 km [Francis, 1974; Drobzhev et al., 1991].

The strongest argument against the AGW model of wave packets, at least for night conditions in summer, is our observations of TWP 1.5 hour before the terminator goes over an observation point and the explicit dependence on the instant of the terminator passage through a magneto-conjugate point. In winter in the north hemisphere, TWPs can be observed 3 hours after the morning ST passage. In equinoxes, TWPs appear after the ST passage without a considerable delay or advance. In summer, TWP can be recorded 1.5-2 hours before the evening ST appearance at an observation point, but at the instant of the ST passage in the magneto-conjugate region. This implies that the TWP formation depends on a number of phenomena at magneto-conjugate points and in the magnetic field line joining these points.

Seasonal dependence and connection with processes in the magneto-conjugate point indicate that MSTWPs have electrodynamic nature. Data from simultaneous optical observations of periodic structures in Japan and Australia also confirm this connection. In recent years, geomagnetic conjugate observations of TIDs using 630-nm airglow imagers were reported. Otsuka et al. (2004) first reported a symmetric pattern of nighttime MSTIDs using 630-nm airglow images obtained at geomagnetic conjugate points in the northern and southern hemispheres. MSTIDs are often observed at the middle latitudes over Japan at night, regardless of geomagnetic activity. These nighttime MSTIDs generally have wavelengths of a few hundred kilometers and propagate southwestward at 50-100 m/s [Shiokawa et al., 2005]. Shiokawa et al. (2005) concluded that the symmetric structures of MSTIDs indicated strong electrodynamic coupling between the two hemispheres through the geomagnetic field line. However it should be noted that all above mentioned papers did not consider the mechanism of generation of studied MSTIDs as a consequence of the movement of the solar terminator.

Ionospheric processes in magneto-conjugate regions have long been studied [Krinberg and Tashchilin, 1984]. However, these investigations did not concern wave processes. The exception was work by Abramchuk et al. (1987). The authors ascertained that the probability of occurrence of the mid-latitude layer Es increased when the terminator passed through the magneto-conjugate region. They advanced the hypothesis allowing the observed phenomenon to be explained by the Alfvén wave propagation along the magnetic field line. But no experimental evidence was given for the recording of corresponding wave process.

Using a new law to the mid-latitude model Sami2 of the ionosphere, Huba et al. (2000) found that ion sound waves can be generated in the topside low-latitude ionosphere at sunrise and sunset. The waves can persist  $\approx 1 - 3$  h at altitudes above the O<sup>+</sup>/H<sup>+</sup> transition altitude ( $\approx 1000$  km) with periods about 10 min. The waves result from the rapid heating and cooling of the lower ionosphere that occurs at sunrise and sunset. At sunrise, photoelectron heating produces strong upward plasma flows along the geomagnetic field. These flows lead to a local compression and heating of the plasma at the apex of the field line, which in turn generates ion sound waves. At sunset, the waves are produced by a rapid cooling of the plasma. According to [Huba et al., 2006], the velocity of wave propagation is about 6 km/s, while the wavelength is close to the length of the corresponding magnetic line.

Our study is the first experimental proof for the correctness of the model [Huba et al., 2000]. Actually, we found out a NEW PHENOMENON and provided the experimental proof for a possible detection of ST-generated ion acoustic waves (oscillation periods of about 20 minutes) using modern methods of ionospheric diagnostics. As such oscillations are sometimes connected with the terminator passage in the ionospheric region conjugated via the geomagnetic field, their transportation by some magnetospheric MHD waves would appear reasonable. Alfvén or slow magneto sonic (SMS) waves propagate along the magnetic field. The periods of the observed oscillations are far beyond the minimum periods of the proper Alfvén waves at these latitudes ( $\approx 10$  s), but correspond to the periods of the first harmonics of stationary SMS waves propagating along geomagnetic

field lines [Leonovich et al., 2006]. In that study the authors conclude that the ionosphere plays no part in either generation or SMS wave absorption. This conclusion stems from the fact that all electromagnetic components and transverse components of plasma oscillations tend to zero in the ionosphere. But the said study also shows that the longitudinal component of the plasma oscillation velocity does not vanish in the ionosphere (also see [Cheremnykh and Parnovsky, 2004]). It is just this oscillation component that is responsible for the electron density modulation that is detected by TEC recording.

Skewness of seasonal dependence in Japan is noteworthy (Fig. 3). In summer, wave packets appear before the sunset, but they are not registered at the winter magneto-conjugate area. This implies that the plasma modulated stream moves in the only one direction - from the winter area after sunset to the summer daytime magneto-conjugate area.

## 7 Conclusion

Main results of this study may be summarized as follows. We obtained the first experimental evidence for the magnetohydrodynamic (MHD) nature of ionospheric medium-scale travelling wave packets (MSTWP). Data were used from total electron content (TEC) measurements made at the dense Japanese network GPS/GEONET (1220 stations) in 2008-2009. The diurnal, seasonal and spectral MSTWP characteristics were found to be specified by the solar terminator (ST) dynamics. MSTWPs are the chain of narrow-band TEC oscillations with single packet's duration of about 1-2 hours and oscillation periods of 10-20 minutes. Its total duration is about 4-6 hours. The MSTWP spatial structure is characterized by the high degree of anisotropy and coherence at the distance of more than 10 wavelengths. MSTWP's direction of travelling is characterized by the high directivity independently of seasons. The daytime MSTWPs occurrence rate is high in winter and during equinoxes. Most of the daytime MSTWPs propagate with the velocity of  $130 \pm 52$  m/s southeastward ( $155 \pm 28^\circ$ ). The nighttime MSTIDs occurrence rate peaks in summer. They propagate at  $110 \pm 43$  m/s southwestward ( $245 \pm 15^\circ$ ). These features are consistent with previous MSTID statistics from 630-nm airglow observations in Japan. In winter, MSTWPs in the northern hemisphere are observed 3-4 hours after the morning ST passage. In summer, MSTWPs are detected 1.5-2 hours before the evening ST occurrence at the observation point, but at the moment of the evening ST passage in the magneto-conjugate area. Both the high Q-factor of oscillatory system and synchronization of MSTWP occurrence with the solar terminator passage at the observation point and in the magneto-conjugate area testify the MHD nature of ST-excited MSTWP generation. The obtained results are the first experimental evidence for the hypothesis of the ST-generated ion sound waves [Huba et al, 2000].

There are many existing and supposed sources of MSAGWs, which make a random interference field of the neutral atmosphere wave disturbance. The result is a random MS intensity distribution of electron density in the ionosphere with chaotic change of the apparent travel direction. This can be recorded some hours before the passage of the morning and evening ST over the observation point or in the magneto-conjugate area. When ST arrives, a strongly regular structure of wave disturbance of MHD origin can be observed. This structure overlaps the random interference field of different sources [Hocke and Schlegel, 1996].

We are aware that this study has revealed only the key averaged patterns of this phenomena, and we hope that it would give impetus to more detailed investigations. However, gaining a better understanding of the formation mechanism for MSTWP disturbances requires modelling and further experimental investigations of the whole process.

Our results are important for the development of ionosphere irregularity physics and modelling of the transionosphere radio wave propagation. The obtained results may be used for development of MSTIDs model necessary for different applications. We should know the time of occurrence of such structures and the direction of wave disturbance front elongation to optimize performance of different satellite radio technical systems. This knowledge is also important for finding possible earthquakes precursors in the given range of TEC oscillation periods, for detecting ionospheric response to hurricanes and tornadoes, etc. Finding the said disturbances that have seismic and meteorological origin is impossible because of the presence of the ST-generated regular wave structure (up to one third of a day).

Spatial-temporal properties and modelling of MSTWP are the aim of our future works.

A new era for studying terminator waves and medium-scale ionospheric disturbances begins: this provides

a better space-time resolution, global observations, and a magnetohydrodynamic conception of nature of these disturbances

## Acknowledgments

The authors thank Profs. A.S. Leonovich, V.A. Mazur and V.M. Somsikov for their interest to the work and fruitful discussion, and Dr. Zhivetiev I.V., Dr. Ding Feng and Prof. S.G. Jin for their assistance in data receiving. We acknowledge the Scripps Orbit and Permanent Array Center (SOPAC), the Crustal Dynamics Data Information System (CDDIS) and GEONET for providing GPS data used in this study. The work was supported by the Interdisciplinary integral project of SB RAS N 56, the RFBR-GFEN grant N 06-05-39026 and RFBR grant 07-05-00127.

## References

- [Abramchuk et al.(1987)] V.P. Abramchuk, V.N. Oraevsky, Yu.Ya. Ruzhin (1987), Sporadic E layer in the twilight period during winter and its relation to sunrise in the conjugate area, *Acta Geod. Geoph. Mont. Hung.*, 22 (1-2), 199–209.
- [Afraimovich (1998)] Afraimovich, E. L. (1998), Palamartchouk, K. S., and Perevalova, N. P., GPS radio interferometry of travelling ionospheric disturbances, *J. Atmos. and Sol.- Terr. Phys.*, 60, N12, 1205–1223.
- [Afraimovich et al.(1999)] Afraimovich, E. L., Boitman, O. N., Zhovty, E. I., et al. (1999), Dynamics and anisotropy of traveling ionospheric disturbances as deduced from transionospheric sounding data, *Radio Sci.*, 34 (2), 477–487.
- [Afraimovich et al.(2003)] Afraimovich, E.L., Perevalova, N.P., Voeikov, S.V. (2003), Traveling wave packets of total electron content disturbances as deduced from global GPS network data, *J. Atm. Solar-Terr. Phys.*, 65(11-13), 1245–1262.
- [Afraimovich(2008)] Afraimovich, E.L. (2008), First GPS-TEC evidence of wave structure excited by solar terminator, *Earth, Planets and Space*, 60, 895–900.
- [Afraimovich et al.(2009)] Afraimovich, E.L., Edemskiy, I.K., Voeykov, S.V., Yasyukevich, Yu.V., Zhivetiev, I.V. (2009), The first GPS-TEC imaging of the space structure of MS wave packets excited by the solar terminator. *Annales Geophysicae*, 27, 1521-1525.
- [Calais et al.(2003)] Calais, E., and J. S. Haase (2003), Detection of ionospheric perturbations using a dense GPS array in Southern California, *Geophys. Res. Lett.*, 50(12), 1628, doi:10.1029/2003GL017708.
- [Cheremnykh et al.(1992)] Cheremnykh, O. K., Parnowski, A. S., Burdo, O. S. (2004), Ballooning modes in the inner magnetosphere of the Earth, *Planetary and Space Science*, 52(13), 1217-1229.
- [Dominici et al.(1997)] Pietro Dominici, Ljiljana, R. Cander and Bruno Zolesi (1997), On the origin of medium-period ionospheric waves and their possible modelling: a short review, *Annali di geofisica*, 11(5), 1171–1178.
- [Drobzhev et al.(1991)] Drobzhev, V. I., M. Z. Kaliyev, Y. G. Litvinov, B. D. Chakenov, and A. F. Yakovets (1991), The spatial coherence of the field of wave disturbances of the ionosphere, *Geomagn. Aeron.*, 31, 334-336.
- [Drobzhev et al.(1992)] Drobzhev, V.I., Zachateisky, D.E., Kozina, P.E., Konoplyanko, M.M., Kurmangaliev, D.A., Somsikov, V.M. (1992), Mid-latitude short-period disturbances in the ionosphere during the solar terminator passage, *Geomagn. Aeron.*, 32, 181-183.
- [Francis et al.(1974)] Francis, S.H. (1974) A theory of medium-scale traveling ionospheric disturbances, *J. Geophys. Res.*, 79, 5245-5259.

- [Dominici et al.(1998)] Galushko, G., Paznukhov, V.V., Yampolski, Y.M., and Foster, J.C. (1998), Incoherent scatter radar observations of AGW/TID events generated by the moving solar terminator, *Ann. Geophys.*, *16*, 821-827.
- [Hernandez-Pajares et al.(2006)] Hernandez-Pajares, M., J. M. Juan, and J. Sanz (2006), Medium-scale traveling ionospheric disturbances affecting GPS measurements: Spatial and temporal analysis, *J. Geophys. Res.*, *111*, A07S11, doi:10.1029/2005JA011474.
- [Hocke et al.(1996)] Hocke, K., and Schlegel, K. (1996), A review of atmospheric gravity waves and traveling ionospheric disturbances: 1982-1995, *Ann. Geophys.*, *14*, 917-940.
- [Huba et al.(2000)] Huba, J.D., Joyce, G., Fedder, J.A. (2000), Ion sound waves in the topside low latitude ionosphere, *Geophysical Research Letters*, *27*(19), 3181-3184.
- [Jacobson et al.(1995)] Jacobson, A. R., R. Carlos, R. S. Massey, and G. Wu (1995), Observations of traveling ionospheric disturbances with a satellite-beacon radio interferometer: Seasonal and local time behavior, *J. Geophys. Res.*, *100*, 1653-1665.
- [Kotake et al.(2007)] Kotake, N., Y. Otsuka, T. Ogawa, T. Tsugawa, and A. Saito (2007), Statistical study of medium-scale traveling ionospheric disturbances observed with the GPS networks in Southern California, *Earth Planets Space*, *59*, 95-102.
- [Krinberg and Tashilin(1984)] Krinberg, I.A., Tashilin, A.V. (1984), *Ionosphere and Plasmosphere*, 188 pp., Nauka, Moscow (in Russian).
- [Dominici et al.(2006)] Leonovich, A.S., Kozlov, D.A., Pilipenko, V.A (2006), Magnetosonic resonance in a dipole-like magnetosphere, *Annales Geophysicae*, *24*(8), 2277-2289.
- [Mercier(1996)] Mercier, C. (1996), Some characteristics of atmospheric gravity waves observed by radio-interferometry, *Annales Geophysicae*, *14*, 42-58.
- [Ogawa et al.(2002)] T. Ogawa, N. Balan, Y. Otsuka, K. Shiokawa, C. Ihara, T. Shimomai, and A. Saito (2002), Observations and modeling of 630 nm airglow and total electron content associated with traveling ionospheric disturbances over Shigaraki, Japan, *Earth Planets Space*, *54*, 45-56, 2002.
- [Otsuka et al.(2004)] Otsuka, Y., K. Shiokawa, T. Ogawa, and P. Wilkinson (2004), Geomagnetic conjugate observations of medium-scale traveling ionospheric disturbances at midlatitude using all-sky airglow imagers, *Geophys. Res. Lett.*, *31*, L15803, doi:10.1029/2004GL020262.
- [Saito et al.(1998)] Saito, A., Fukao, S., and Miyazaki, S. (1998), High resolution mapping of TEC perturbations with the GSI GPS network over Japan, *Geophys. Res. Lett.*, *25*, 3079-3082.
- [Shiokawa et al.(2003)] Shiokawa, K., Otsuka, Y., Ihara, C., Ogawa, T., and Rich, F. J. (2003) Ground and satellite observations of nighttime medium-scale traveling ionospheric disturbance at midlatitude, *J. Geophys. Res.*, *108*, S1A 3-1, doi:10.1029/2002JA009639.
- [Shiokawa et al.(2005)] Shiokawa, K., Otsuka, Y., Tsugawa, T., Ogawa, T., Saito, A., Ohshima, K., Kubota, M., Maruyama, T., Nakamura, T., Yamamoto, M., and Wilkinson, P. (2005), Geomagnetic conjugate observation of nighttime medium- and large-scale traveling ionospheric disturbances: FRONT3 campaign, *J. Geophys. Res.*, *V. 110*, A05303, doi:10.1029/2004JA010845.
- [Somsikov(1995)] Somsikov, V. M. (1995), On mechanisms for the formation of atmospheric irregularities in the solar terminator region, *J. Atmos. Terr. Phys.*, *57*(1), 75-83.
- [Tsugawa et al.(2007)] Tsugawa T., Otsuka, Y., Coster, A.J., Saito, A., Medium-scale traveling ionospheric disturbances detected with dense and wide TEC maps over North America, *Geophys. Res. Lett.*, *34*, L22101, doi:10.1029/2007GL031663.